Comparison of Hard Vaporization and Soft Ionization Techniques in the Mass Spectrometry of some Palladium(II) and Platinum(II) Complexes with C-bonded Heterocyclic Ligands

R. BERTANI*

Centro di Chimica e Tecnologia dei Composti Metallorganici degli Elementi di Transizione, C.N.R., via Marzolo 9, Padua (Italy)

W. CECCHETTO, R. POLLONI

Dipartimento di Spettroscopia, Elettrochimica e Chimica Fisica, Università di Venezia, Venice (Italy)

B. CROCIANI

Dipartimento di Chimica Inorganica, Università di Palermo (Italy)

R. SERAGLIA and P. TRALDI

Servizio di Spettrometria di Massa, C.N.R., viale Stati Uniti 4, Padua (Italy)

(Received December 12, 1989; revised February 9, 1990)

Abstract

Electron impact, fast atom bombardment and laser induced vaporization techniques are compared in the mass spectrometric behaviour of some palladium(II) and platinum(II) complexes with C-bonded heterocyclic ligands of the type *trans*-[MCl(R_N)(PPh_3)$_2$] [M = Pd, R_N = 2-pyridyl, **1**; 2-pyrazyl, **2**; 2-pyrimidyl, **3**; M = Pt, R_N = 2-pyridyl, **4**].

Introduction

New mass spectrometric methods were recently used to obtain mass spectra of organometallic compounds. Conventional electron impact (EI) mass spectrometry has long been employed in the analysis and characterization of organometallic and inorganic molecules, but severe limitations emerged when applied to ionic materials, high molecular weight metal clusters and thermolabile compounds. The fast atom bombardment (FAB) technique considerably increased the range of compounds which could be studied by mass spectrometry, including salts and poorly volatile materials [1].

Recently, exciting results were obtained by laser induced vaporization (LIV) mass spectrometry, where a 'hard' controlled vaporization of the samples is obtained [2, 3].

Here we use the FAB, LIV and EI techniques for the characterization of some organometallic compounds of palladium(II) and platinum(II) (**1**–**4**) with 2-C-bonded heteroaromatic ligands, in order to compare the gas phase results.

Experimental

The compounds *trans*-[MCl(R_N)(PPh_3)$_2$] [M = Pd, R_N = 2-pyridyl, **1**; 2-pyrazyl, **2**; 2-pyrimidyl, **3**; M = Pt, R_N = 2-pyridyl, **4**] were prepared according to literature methods [4, 5].

Mass spectrometric measurements were performed on a VG ZAB 2F instrument [6] operating in EI conditions (70 eV, 200 μA). The samples were introduced either by the usual insertion probe, or by the optic fiber probe previously described [2]. A ruby laser was employed with an output energy of about 3J. FAB spectra were obtained by bombarding glycerol or thioglycerol solutions of the samples by 8 keV Xe atoms [7]. Metastable transitions were detected by B/E linked scans [8] which are marked by asterisks in the Schemes.

Exact mass measurements for all metal-containing fragment ions were obtained with the peak matching technique at 30 000 resolving power (10% valley definition).

Results and Discussion

EI mass spectra of compounds **1**–**4** demonstrate the occurrence of severe thermal decomposition, the higher mass ions at *m/z* 262 and 183 being related to the phosphino moiety, as is shown by the isotopic pattern, and are therefore ineffective in structural

*Author to whom correspondence should be addressed.

0020-1693/90/$3.50

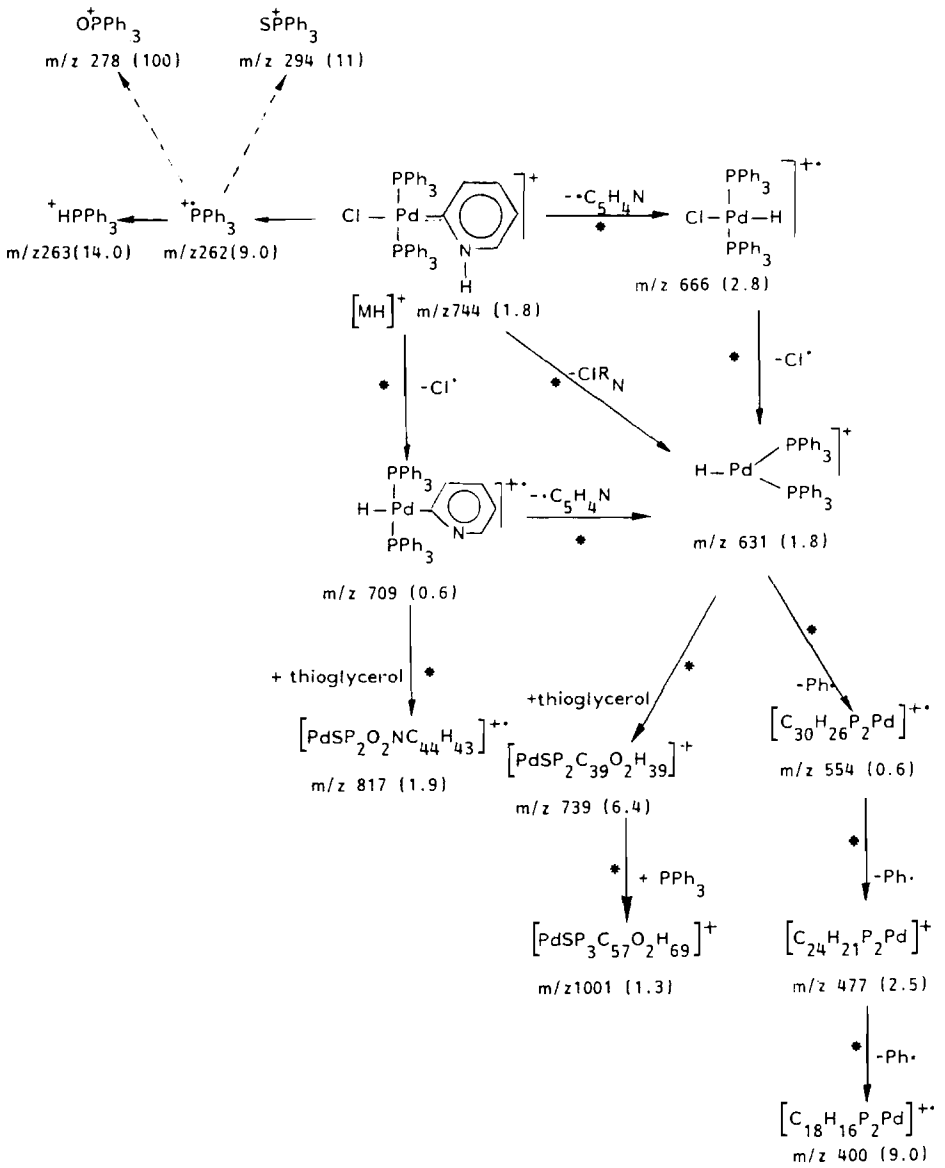

Scheme 1. FAB fragmentation pathways for compound **1**. The *m/z* values are referred to ^{106}Pd and ^{35}Cl isotopes.

characterization of **1**–**4**. The palladium compounds **1**–**3** exhibit closely related positive FAB spectra in thioglycerol, which is found to be the most suitable matrix.

As an example, the fragmentation pattern of **1** is reported in Scheme 1. The spectra involve the fragmentation of the N-protonated derivatives of compounds **1**–**3**, due to proton transfer from the matrix to the 1-nitrogen atom of the heterocycle group R_N, whose basicity is strongly enhanced by the *trans*-$MCl(PPh_3)_2$ substituent [5]. The N-protonation is confirmed by the fact that identical FAB spectra are observed for the 1-N-protonated cationic complexes *trans*-$[PdCl(R_N\text{-}H)(PPh_3)_2]ClO_4$, independently prepared [5, 9, 10].

Low abundance peaks corresponding to $[M + H]^+$ ions at *m/z* 744 for **1** and *m/z* 745 for **2** and **3**, respectively, are present (Table 1). A peak at *m/z* 631 corresponding to ions $[HPd(PPh_3)_2]^+$ derived from the elimination of ClR_N, is also present with abundances of *c.* 1.8% for **1**, 0.6% for **2** and 0.3% for **3**.

Loss of the R_N radical also occurs and gives rise to ions at *m/z* 666 for **1**–**3**, with relative abundances of *c* 2.8% for **1**, 1.6% for **2** and 0.9% for **3**.

It is noteworthy that the relative abundances of $[MH - R_N]^{+\cdot}$ and $[MH - ClR_N]^+$ ions depend on the R_N ligand in the order 2-pyrimidyl < 2-pyrazyl < 2-pyridyl. This may be related to a decreasing metal–carbon bond strength from 2-pyrimidyl to 2-pyridyl derivative, owing to changes in the $d_\pi \rightarrow \pi^*$ back-

TABLE 1. FAB mass spectra of compounds 1–4 [*m/z* (rel.ab.%)] in thioglycerol

Compound 1: 183(18.0), 184(4.0), 185(3.0), 201(31.0), 202(6.0), 262(9.0), 263(14.0), 264(3.0), 276(5.0), 277(5.0), 278(100.0), 279(33.0), 289(4.0), 290(4.0), 291(7.0), 292(2.0), 293(4.0), 294(11.0), 295(2.0), 296(2.0), 317(1.0), 318(2.0), 319(2.5), 320(3.0), 321(3.0), 322(2.5), 323(2.0), 342(1.5), 325(1.0), 339(10.0), 340(12.0), 341(13.0), 367(3.0), 368(3.0), 369(9.0), 370(3.0), 393(2.0), 394(4.0), 395(7.0), 396(8.0), 397(3.0), 398(6.0), 399(8.0), 400(9.0), 401(5.0), 411(2.0), 444(1.0), 445(3.0), 446(5.0), 447(2.0), 448(3.0), 449(1.0), 450(1.0), 473(1.5), 474(1.5), 475(2.0), 476(2.0), 477(2.5), 478(1.0), 479(1.0), 480(0.5), 539(2.0), 540(5.0), 541(6.0), 542(7.0), 543(6.0), 544(8.0), 545(5.0), 546(6.0), 547(3.0), 548(3.0), 552(0.5), 553(0.5), 554(0.6), 555(0.3), 580(1.0), 581(1.0), 582(1.5), 583(2.0), 584(2.0), 585(1.5), 586(1.5), 587(1.0), 588(1.0), 627(0.5), 628(1.2), 629(1.5), 630(1.6), 631(1.8), 632(1.8), 633(1.0), 634(1.3), 635(0.4), 636(0.5), 655(0.3), 656(0.5), 657(1.1), 658(1.4), 659(1.8), 660(1.7), 661(2.0), 662(1.5), 663(1.5), 664(0.9), 665(1.7), 666(2.8), 667(0.5), 668(0.3), 706(0.2), 707(0.2), 708(0.3), 709(0.6), 710(0.1), 731(0.2), 732(0.5), 733(1.2), 734(2.9), 735(4.3), 736(5.4), 737(5.4), 738(6.0), 739(6.4), 740(4.4), 741(3.3), 742(2.0), 743(1.5), 744(1.8), 745(0.4), 810(0.2), 811(0.5), 812(0.9), 813(1.2), 814(1.3), 815(1.3), 816(1.5), 817(1.9), 818(1.1), 819(0.5), 820(0.4), 821(0.2), 840(0.1), 841(0.1), 842(0.2), 843(0.3), 844(0.4), 845(0.5), 846(0.4), 847(0.5), 848(0.4), 849(0.4), 850(0.2), 851(0.2), 996(0.3), 997(0.7), 998(0.9), 999(1.1), 1000(1.1), 1001(1.3), 1002(0.9), 1003(0.1), 1004(0.5), 1005(0.4), 1006(0.2).

Compound 2[a]: 183(68.0), 184(12.0), 185(25.0), 186(5.0), 201(30.0), 202(7.0), 262(15.0), 263(54.0), 264(10.0), 265(2.0), 279(100.0), 280(21.0), 281(4.0), 295(40.0), 296(8.0), 297(3.0), 339(20.0), 340(5.0), 341(9.0), 342(2.0), 343(1.0), 368(4.0), 369(4.0), 370(2.7), 371(7.0), 372(4.0), 373(2.0), 394(2.0), 395(3.5), 396(6.0), 397(6.5), 398(8.0), 399(6.5), 400(8.0), 401(7.0), 402(1.5), 403(3.0), 630(0.6), 631(0.6), 632(0.6), 633(0.6), 634(0.6), 635(0.6), 636(0.1), 658(0.3), 659(0.4), 660(0.5), 661(0.5), 662(1.0), 663(0.8), 664(1.6), 665(1.4), 666(1.6), 667(0.4), 668(0.2), 708(0.1), 709(0.3), 710(0.4), 711(0.2), 712(0.1), 734(0.2), 735(0.4), 736(0.4), 737(0.6), 738(0.5), 739(0.7), 740(0.4), 741(0.6), 742(0.2), 743(0.3), 744(0.3), 745(0.4), 746(0.1), 747(0.1).

Compound 3[a]: 180(35.0), 181(4.0), 182(45.0), 183(5.0), 184(17.0), 185(2.0), 186(7.0), 196(5.0), 197(10.0), 198(63.0), 199(7.0), 200(18.0), 201(2.0), 201(21.0), 203(2.0), 214(5.0), 215(70.0), 216(100), 217(21.0), 218(100.0), 219(12.0), 220(15.0), 233(10.0), 257(5.0), 253(1.5), 263(10.0), 264(12.0), 280(67.0), 281(16.0), 295(11.0), 296(95.0), 297(23.0), 298(7.0), 322(8.0), 323(2.0), 324(18.0), 325(3.0), 326(6.0), 370(26.0), 371(6.0), 372(2.0), 398(0.1), 399(0.1), 400(0.2), 401(0.1), 402(0.1), 430(22.0), 431(4.0), 432(5.0), 446(4.0), 447(3.0), 448(3.0), 449(2.0), 450(2.0), 451(1.0), 452(1.0), 472(3.0), 482(3.0), 552(0.5), 553(0.6), 554(0.8), 555(0.7), 556(0.9), 557(0.6), 558(0.7), 559(0.3), 560(0.3), 630(0.3), 631(0.3), 632(0.3), 633(0.4), 634(0.3), 635(0.3), 636(0.3), 637(0.2), 644(1.0), 645(0.6), 646(0.9), 647(0.5), 648(0.7), 649(0.4), 650(0.3), 658(0.2), 659(0.4), 660(0.5), 661(0.5), 662(0.7), 663(0.7), 664(0.8), 665(0.8), 666(0.9), 667(0.3), 668(0.3), 707(0.1), 708(0.2), 709(0.2), 710(0.7), 711(0.2), 712(0.1), 713(0.1), 734(0.3), 735(0.3), 736(0.6), 737(0.5), 738(0.7), 739(0.7), 740(0.7), 741(0.6), 742(0.5), 743(0.5), 744(0.5), 745(0.6), 746(0.2), 750(0.2), 751(0.2), 752(1.0), 753(1.8), 754(2.9), 755(1.2), 756(2.3), 757(0.9), 758(1.3), 759(0.4), 760(0.2).

Compound 4[b]: 181(50.0), 182(2.0), 183(100.0), 184(10.0), 185(3.0), 186(1.0), 187(2.0), 262(10.0), 263(20.0), 264(8.0), 265(1.0), 277(2.0), 278(8.0), 279(2.0), 280(4.0), 299(1.0), 300(3.0), 301(4.0), 302(6.0), 303(6.0), 304(5.0), 305(2.0), 306(3.0), 375(1.0), 376(1.0), 377(3.0), 378(4.0), 379(7.0), 380(1.0), 381(2.0), 453(1.0), 454(1.0), 455(3.0), 456(3.5), 457(2.5), 458(2.0), 459(2.0), 460(1.0), 530(0.7), 531(1.0), 532(2.2), 533(2.0), 534(2.5), 534(2.5), 535(2.5), 536(2.1), 537(0.8), 538(0.7), 539(0.2), 568(0.2), 569(0.4), 570(0.6), 571(0.1), 717(0.5), 718(1.0), 719(1.5), 720(0.5), 721(0.5), 722(0.5), 723(0.5), 751(0.2), 752(0.9), 753(0.5), 754(1.0), 755(0.4), 756(0.2), 757(0.2), 758(0.2), 795(1.0), 796(2.0), 797(2.2), 798(1.5), 799(1.0), 800(0.5), 828(0.3), 829(0.7), 830(0.5), 831(0.8), 832(1.0), 833(0.6), 834(0.2), 979(0.2), 980(0.5), 981(0.3), 982(0.2), 983(0.1).

[a]Differences in M^+ clusters are due to partial overlapping with ions at *m/z* 739. [b]Ions at *m/z* 980 are due to species $[Pt(PPh_3)_3]^+$ (see Scheme 2).

donation. In the N-protonated systems, a significant contribution of the carbene-like limiting structure

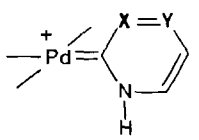

X = Y = CH (2-pyridyl)
X = CH, Y = N (2-pyrazyl)
X = N, Y = CH (2-pyrimidyl)

through a $d_\pi \rightarrow \pi^+$ backbonding from the metal to the ligand was suggested by ^1H and ^{13}C NMR studies [9, 10].

In the FAB spectrum of **1**, sequential losses of the phenyl radical from ions at *m/z* 631 are observed and some metal-containing ions are found to react with the matrix. As an example, the well detectable ionic species at *m/z* 739 and 817 arise from thioglycerol addition to the ions at *m/z* 631 and 709, respectively. Further reaction of ions at 739 with PPh_3 leads to ions at *m/z* 1001. More complex reactions are likely to occur between free triphenylphosphine and thioglycerol involving formation of the ions at *m/z* 278 and 294, corresponding to phosphine oxide and phosphine sulfide. The main features of the fragmentation pathway arising from the ions at *m/z* 631 are also observed for compounds **2** and **3**. In these cases, however, the resulting ions appear with markedly lower abundances.

Complexes **1**–**3** exhibit fragmentation pathways which parallel those reported for other phosphino complexes of Pd(II) [11] under FAB conditions, as far as the ions at *m/z* 631 are concerned. The only

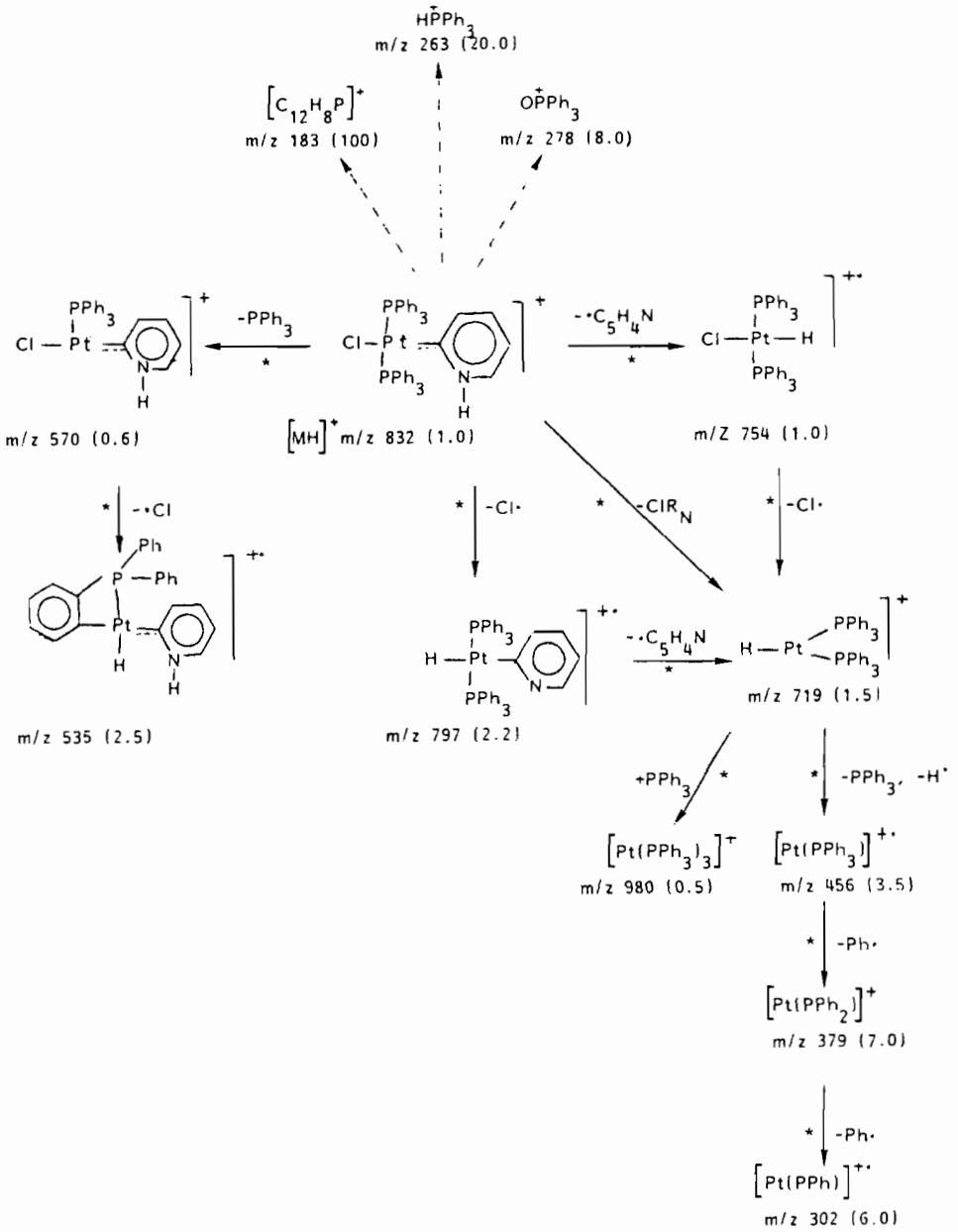

Scheme 2. FAB fragmentation pathways for compound **4**. The *m/z* values are referred to ^{194}Pt and ^{35}Cl isotopes.

difference in the present systems is the addition of the matrix to some metal-containing ions, as reported above.

Under FAB conditions, complexes **1**–**3** do not undergo dimerization to the binuclear species $[PdCl(\mu\text{-}R_N)(PPh_3)]_2$ (μ-R_N = C,N-bridging ligands) as occurs in chlorinated solvents [4].

The positive FAB spectrum of compound **4** in glycerol matrix (Scheme 2) shows the $[M+H]^+$ ions at *m/z* 832, which lose PPh_3 and $Cl^\cdot$ with formation of the ions at *m/z* 570 and 797, respectively. Loss of the 2-pyridyl radical also occurs generating ions at *m/z* 754, while the elimination of 2-chloropyridine gives rise to ions at *m/z* 719. The fragmentation pattern is substantially similar to that of compound **1**. For **4**, however, no addition product of glycerol to metal-containing fragments is detected. The results obtained in thioglycerol are very poor, due to the lower solubility of **4** in such a matrix.

Finally, LIV spectra of **1**–**4** (Table 2) show molecular ions in low abundances, which undergo loss of the heterocyclic radical and also reductive elimination of ClR_N. Under these conditions no protonation of 2-C-bonded heterocyclic ligands occurs. The relative abundances of ions at *m/z* 630 are *c.* 5.0% for **1**, 3.0% for **2** and 1.8% for **3**, i.e. in

the same trend as in the FAB spectra. This result suggests that the Pd–R_N bond strength in the neutral complexes decreases in the same order (R_N = 2-pyrimidyl > 2-pyrazyl > 2-pyridyl) observed for the corresponding N-protonated derivatives. This is also the case for the relative abundances of the ions arising from loss of $\cdot R_N$: *m/z* 665, *c.* 3.0% for **1**, 2.5% for **2** and 1.5% for **3**. It is noteworthy that in the LIV mass spectra of **1**–**3** particularly abundant metal-containing ions with the 2-C-bonded heterocyclic group are present, which undergo fragmentation pathways different from those observed in the FAB spectra. In the LIV spectrum of **1**, ions at *m/z* 184 (11%) are due to the species $[Pd(2\text{-pyridyl})]^+$ as proved by isotopic analysis. Likewise, in the spectra of **2** and **3** the $[Pd(2\text{-pyrazyl})]^+$ and $[Pd(2\text{-pyrimidyl})]^+$ ions are detected at *m/z* 185 in both cases. The LIV fragmentation pattern of **3** (Scheme 3) shows also the metal-containing ions at *m/z* 443 which result from breaking of the pyrimidyl group.

The LIV spectrum of **4** shows ions at *m/z* 831 of low abundance, which lose $\cdot R_N$ and 2-Cl-pyridine giving rise to ions at *m/z* 753 and 718, respectively. Loss of a phenyl radical from the ions at *m/z* 718 yields the ionic fragments at *m/z* 641. For the latter ions, a similar fragmentation pattern is observed under EI conditions for other Pt(II) complexes containing the *trans*-PPh_3–Pt–PPh_3 unit [12].

As a general remark, in LIV conditions the production of metal-containing ions is strongly enhanced, which suggests that the energy deposition in molecular species is somehow lower than under FAB conditions.

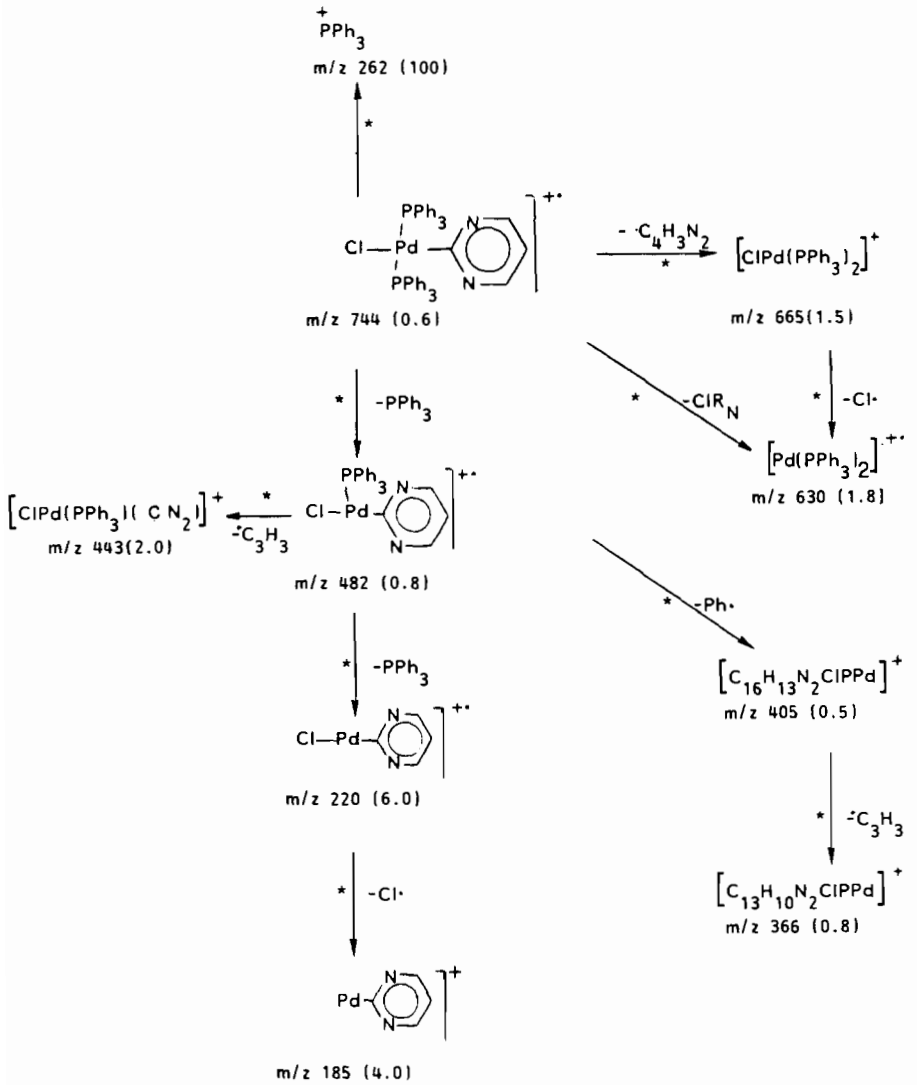

Scheme 3. LIV fragmentation pathways for compound **3**. The *m/z* values are referred to ^{106}Pd and ^{35}Cl isotopes.

TABLE 2. Laser induced vaporization mass spectra of compounds **1**–**4**·

Compound **1**: 179(0.2), 180(0.2), 181(0.5), 182(0.8), 183(1.5), 184(1.1), 185(0.2), 186(0.2), 187(0.1), 256(1.0), 257(8.0), 258(2.0), 259(8.0), 260(10.0), 261(80.0), 262(100.0), 263(80.0), 264(50.0), 265(5.0), 266(2.0), 626(1.0), 627(1.0), 628(2.0), 629(3.0), 630(5.0), 631(0.5), 632(0.2), 633(0.2), 634(0.1), 663(0.7), 664(0.8), 665(3.0), 666(0.5), 667(0.5), 668(0.2), 669(0.2), 741(0.2), 742(0.3), 743(0.5), 744(0.2), 745(0.4), 746(0.1).

Compound **2**: 181(0.2), 182(0.5), 183(2.0), 184(3.0), 185(2.0), 186(1.0), 187(0.8), 188(0.2), 189(0.2), 261(80.0), 262(100.0), 263(20.0), 479(0.2), 480(0.3), 481(0.5), 482(0.2), 483(0.1), 629(3.8), 630(3.0), 631(3.0), 632(1.5), 633(1.5), 634(0.2), 635(0.2), 662(1.8), 663(2.0), 664(2.1), 665(2.5), 666(1.2), 667(0.2), 668(0.2), 741(0.2), 742(0.2), 743(0.3), 744(0.5), 745(0.2), 746(0.4), 747(0.1).

Compound **3**: 181(0.5), 182(1.0), 183(1.5), 184(3.0), 185(4.0), 186(2.0), 187(1.0), 188(1.0), 189(0.5), 190(0.5), 214(0.5), 215(1.0), 216(1.0), 217(2.0), 218(4.0), 219(5.0), 220(6.0), 221(3.0), 222(2.0), 223(1.0), 224(1.0), 258(1.0), 259(1.0), 260(5.0), 261(80.0), 262(100.0), 263(70.0), 264(10.0), 265(10.0), 266(1.0), 267(1.0), 363(0.2), 364(0.5), 365(0.6), 366(0.8), 367(0.3), 368(0.1), 402(0.2), 403(0.2), 404(0.3), 405(0.5), 406(0.2), 437(0.5), 438(0.5), 439(1.0), 440(1.5), 441(1.8), 442(1.8), 443(2.0), 444(0.5), 445(0.2), 446(0.2), 478(0.2), 479(0.4), 480(0.4), 481(0.4), 482(0.8), 483(0.2), 484(0.2), 627(0.5), 628(1.0), 629(1.3), 630(1.8), 631(1.7), 632(0.8), 633(0.2), 634(0.2), 662(0.2), 663(0.4), 664(1.5), 665(1.5), 666(0.2), 740(0.2), 741(0.2), 742(0.3), 743(0.5), 744(0.6), 745(0.2), 746(0.4), 747(0.1).

Compound **4**: 257(1.0), 258(5.0), 259(1.0), 260(5.0), 261(80.0), 262(100.0), 263(60.0), 264(20.0), 265(1.0), 266(71.0), 378(0.3), 379(1.0), 380(0.8), 381(0.6), 455(0.3), 456(1.0), 457(0.5), 458(0.3), 459(0.3), 639(0.7), 640(0.8), 641(0.8), 642(1.0), 643(0.5), 644(0.7), 645(0.5), 646(0.1), 647(0.3), 716(0.2), 717(0.2), 718(0.8), 719(0.5), 720(0.4), 721(0.1), 750(0.2), 751(0.8), 752(0.4), 753(0.2), 754(1.0), 755(0.3), 756(0.2), 828(0.2), 829(0.4), 830(0.4), 831(0.5), 832(0.2), 833(0.4), 834(0.2).

Acknowledgement

Financial support from the Ministero Pubblica Istruzione (Research Fund 60%) is gratefully acknowledged.

References

1 M. I. Bruce and M. J. Liddell, *Appl. Organomet. Chem., 1* (1987) 192.
2 W. Cecchetto, R. Polloni, A. M. Maccioni and P. Traldi, *Org. Mass Spectrom., 21* (1986) 517.
3 R. Bertani, P. Traldi, W. Cecchetto and R. Polloni, *Inorg. Chim. Acta, 143* (1987) 27.
4 R. Bertani, A. Berton, F. di Bianca and B. Crociani, *J. Organomet. Chem., 303* (1986) 283.
5 B. Crociani, F. Di Bianca, A. Giovenco, A. Berton and R. Bertani, *J. Organomet. Chem., 361* (1989) 255.
6 R. P. Morgan, J. H. Beynon, R. H. Bateman and B. N. Green, *Int. J. Mass Spectrom. Ion Phys., 28* (1979) 171.
7 (a) J. M. Miller, *Adv. Inorg. Chem. Radiochem., 28* (1984) 1; (b) D. H. Williams, A. F. Findeis, S. Naylor and B. W. Gibson, *J. Am. Chem. Soc., 109* (1987) 1980.
8 A. P. Bruins, K. R. Jennings and S. Evans, *Int. J. Mass Spectrom. Ion Phys., 26* (1978) 395.
9 B. Crociani, F. Di Bianca, A. Giovenco and A. Scrivanti, *J. Organomet. Chem., 251* (1983) 393.
10 B. Crociani, F. Di Bianca, A. Giovenco and A. Scrivanti, *J. Organomet. Chem., 291* (1985) 259.
11 A. Asker, A. M. Greenway, K. R. Seddom and A. A. Shimaran, *J. Organomet. Chem., 354* (1988) 257.
12 R. Bertani, A. M. Maccioni, P. Traldi and G. Carturan, *Inorg. Chim. Acta, 121* (1986) 147.